

Search for the decay $\chi_{c1}(3872) \rightarrow \pi^+\pi^-\chi_{c1}$

M. Ablikim¹, M. N. Achasov^{4,b}, P. Adlarson⁷⁵, X. C. Ai⁸¹, R. Aliberti³⁵, A. Amoroso^{74A,74C}, M. R. An³⁹, Q. An^{71,58}, Y. Bai⁵⁷, O. Bakina³⁶, I. Balossino^{29A}, Y. Ban^{46,g}, H.-R. Bao⁶³, V. Batozskaya^{1,44}, K. Begzsuren³², N. Berger³⁵, M. Berlowski⁴⁴, M. Bertani^{28A}, D. Bettoni^{29A}, F. Bianchi^{74A,74C}, E. Bianco^{74A,74C}, A. Bortone^{74A,74C}, I. Boyko³⁶, R. A. Briere⁵, A. Brueggemann⁶⁸, H. Cai⁷⁶, X. Cai^{1,58}, A. Calcaterra^{28A}, G. F. Cao^{1,63}, N. Cao^{1,63}, S. A. Cetin^{62A}, J. F. Chang^{1,58}, T. T. Chang⁷⁷, W. L. Chang^{1,63}, G. R. Che⁴³, G. Chelkov^{36,a}, C. Chen⁴³, Chao Chen⁵⁵, G. Chen¹, H. S. Chen^{1,63}, M. L. Chen^{1,58,63}, S. J. Chen⁴², S. L. Chen⁴⁵, S. M. Chen⁶¹, T. Chen^{1,63}, X. R. Chen^{31,63}, X. T. Chen^{1,63}, Y. B. Chen^{1,58}, Y. Q. Chen³⁴, Z. J. Chen^{25,h}, S. K. Choi^{10A}, X. Chu⁴³, G. Cibinetto^{29A}, S. C. Coen³, F. Cossio^{74C}, J. J. Cui⁵⁰, H. L. Dai^{1,58}, J. P. Dai⁷⁹, A. Dbeyssi¹⁸, R. E. de Boer³, D. Dedovich³⁶, Z. Y. Deng¹, A. Denig³⁵, I. Denysenko³⁶, M. Destefanis^{74A,74C}, F. De Mori^{74A,74C}, B. Ding^{66,1}, X. X. Ding^{46,g}, Y. Ding⁴⁰, Y. Ding³⁴, J. Dong^{1,58}, L. Y. Dong^{1,63}, M. Y. Dong^{1,58,63}, X. Dong⁷⁶, M. C. Du¹, S. X. Du⁸¹, Z. H. Duan⁴², P. Egorov^{36,a}, Y. H. Fan⁴⁵, J. Fang^{1,58}, S. S. Fang^{1,63}, W. X. Fang¹, Y. Fang¹, Y. Q. Fang^{1,58}, R. Farinelli^{29A}, L. Fava^{74B,74C}, F. Feldbauer³, G. Felici^{28A}, C. Q. Feng^{71,58}, J. H. Feng⁵⁹, K. Fischer⁶⁹, M. Fritsch³, C. D. Fu¹, J. L. Fu⁶³, Y. W. Fu¹, H. Gao⁶³, Y. N. Gao^{46,g}, Yang Gao^{71,58}, S. Garbolino^{74C}, I. Garzia^{29A,29B}, P. T. Ge⁷⁶, Z. W. Ge⁴², C. Geng⁵⁹, E. M. Gersabeck⁶⁷, A. Gilman⁶⁹, K. Goetzen¹³, L. Gong⁴⁰, W. X. Gong^{1,58}, W. Gradl³⁵, S. Gramigna^{29A,29B}, M. Greco^{74A,74C}, M. H. Gu^{1,58}, Y. T. Gu¹⁵, C. Y. Guan^{1,63}, Z. L. Guan²², A. Q. Guo^{31,63}, L. B. Guo⁴¹, M. J. Guo⁵⁰, R. P. Guo⁴⁹, Y. P. Guo^{12,f}, A. Guskov^{36,a}, J. Gutierrez²⁷, T. T. Han¹, W. Y. Han³⁹, X. Q. Hao¹⁹, F. A. Harris⁶⁵, K. K. He⁵⁵, K. L. He^{1,63}, F. H. Heinsius³, C. H. Heinz³⁵, Y. K. Heng^{1,58,63}, C. Herold⁶⁰, T. Holtmann³, P. C. Hong^{12,f}, G. Y. Hou^{1,63}, X. T. Hou^{1,63}, Y. R. Hou⁶³, Z. L. Hou¹, B. Y. Hu⁵⁹, H. M. Hu^{1,63}, J. F. Hu^{56,i}, T. Hu^{1,58,63}, Y. Hu¹, G. S. Huang^{71,58}, K. X. Huang⁵⁹, L. Q. Huang^{31,63}, X. T. Huang⁵⁰, Y. P. Huang¹, T. Hussain⁷³, N. Hüsken^{27,35}, N. in der Wiesche⁶⁸, M. Irshad^{71,58}, J. Jackson²⁷, S. Jaeger³, S. Janchiv³², J. H. Jeong^{10A}, Q. Ji¹, Q. P. Ji¹⁹, X. B. Ji^{1,63}, X. L. Ji^{1,58}, Y. Y. Ji⁵⁰, X. Q. Jia⁵⁰, Z. K. Jia^{71,58}, H. J. Jiang⁷⁶, P. C. Jiang^{46,g}, S. S. Jiang³⁹, T. J. Jiang¹⁶, X. S. Jiang^{1,58,63}, Y. Jiang⁶³, J. B. Jiao⁵⁰, Z. Jiao²³, S. Jin⁴², Y. Jin⁶⁶, M. Q. Jing^{1,63}, X. M. Jing⁶³, T. Johansson⁷⁵, X. K.¹, S. Kabana³³, N. Kalantar-Nayestanaki⁶⁴, X. L. Kang⁹, X. S. Kang⁴⁰, M. Kavatsyuk⁶⁴, B. C. Ke⁸¹, V. Khachatryan²⁷, A. Khoukaz⁶⁸, R. Kiuchi¹, R. Kliemt¹³, O. B. Kolcu^{62A}, B. Kopf³, M. Kuessner³, A. Kupsc^{44,75}, W. Kühn³⁷, J. J. Lane⁶⁷, P. Larin¹⁸, A. Lavania²⁶, L. Lavezzi^{74A,74C}, T. T. Lei^{71,58}, Z. H. Lei^{71,58}, H. Leithoff³⁵, M. Lellmann³⁵, T. Lenz³⁵, C. Li⁴⁷, C. Li⁴³, C. H. Li³⁹, Cheng Li^{71,58}, D. M. Li⁸¹, F. Li^{1,58}, G. Li¹, H. Li^{71,58}, H. B. Li^{1,63}, H. J. Li¹⁹, H. N. Li^{56,i}, Hui Li⁴³, J. R. Li⁶¹, J. S. Li⁵⁹, J. W. Li⁵⁰, Ke Li¹, L. J Li^{1,63}, L. K. Li¹, Lei Li⁴⁸, M. H. Li⁴³, P. R. Li^{38,k}, Q. X. Li⁵⁰, S. X. Li¹², T. Li⁵⁰, W. D. Li^{1,63}, W. G. Li¹, X. H. Li^{71,58}, X. L. Li⁵⁰, Xiaoyu Li^{1,63}, Y. G. Li^{46,g}, Z. J. Li⁵⁹, Z. X. Li¹⁵, C. Liang⁴², H. Liang^{1,63}, H. Liang^{71,58}, Y. F. Liang⁵⁴, Y. T. Liang^{31,63}, G. R. Liao¹⁴, L. Z. Liao⁵⁰, Y. P. Liao^{1,63}, J. Libby²⁶, A. Limphirat⁶⁰, D. X. Lin^{31,63}, T. Lin¹, B. J. Liu¹, B. X. Liu⁷⁶, C. Liu³⁴, C. X. Liu¹, F. H. Liu⁵³, Fang Liu¹, Feng Liu⁶, G. M. Liu^{56,i}, H. Liu^{38,j,k}, H. B. Liu¹⁵, H. M. Liu^{1,63}, Huanhuan Liu¹, Huihui Liu²¹, J. B. Liu^{71,58}, J. Y. Liu^{1,63}, K. Liu¹, K. Y. Liu⁴⁰, Ke Liu²², L. Liu^{71,58}, L. C. Liu⁴³, Lu Liu⁴³, M. H. Liu^{12,f}, P. L. Liu¹, Q. Liu⁶³, S. B. Liu^{71,58}, T. Liu^{12,f}, W. K. Liu⁴³, W. M. Liu^{71,58}, X. Liu^{38,j,k}, Y. Liu⁸¹, Y. Liu^{38,j,k}, Y. B. Liu⁴³, Z. A. Liu^{1,58,63}, Z. Q. Liu⁵⁰, X. C. Lou^{1,58,63}, F. X. Lu⁵⁹, H. J. Lu²³, J. G. Lu^{1,58}, X. L. Lu¹, Y. Lu⁷, Y. P. Lu^{1,58}, Z. H. Lu^{1,63}, C. L. Luo⁴¹, M. X. Luo⁸⁰, T. Luo^{12,f}, X. L. Luo^{1,58}, X. R. Lyu⁶³, Y. F. Lyu⁴³, F. C. Ma⁴⁰, H. Ma⁷⁹, H. L. Ma¹, J. L. Ma^{1,63}, L. L. Ma⁵⁰, M. M. Ma^{1,63}, Q. M. Ma¹, R. Q. Ma^{1,63}, X. Y. Ma^{1,58}, Y. Ma^{46,g}, Y. M. Ma³¹, F. E. Maas¹⁸, M. Maggiora^{74A,74C}, S. Malde⁶⁹, Q. A. Malik⁷³, A. Mangoni^{28B}, Y. J. Mao^{46,g}, Z. P. Mao¹, S. Marcello^{74A,74C}, Z. X. Meng⁶⁶, J. G. Messchendorp^{13,64}, G. Mezzadri^{29A}, H. Miao^{1,63}, T. J. Min⁴², R. E. Mitchell²⁷, X. H. Mo^{1,58,63}, B. Moses²⁷, N. Yu. Muchnoi^{4,b}, J. Muskalla³⁵, Y. Nefedov³⁶, F. Nerling^{18,d}, I. B. Nikolaev^{4,b}, Z. Ning^{1,58}, S. Nisar^{11,l}, Q. L. Niu^{38,j,k}, W. D. Niu⁵⁵, Y. Niu⁵⁰, S. L. Olsen⁶³, Q. Ouyang^{1,58,63}, S. Pacetti^{28B,28C}, X. Pan⁵⁵, Y. Pan⁵⁷, A. Pathak³⁴, P. Patteri^{28A}, Y. P. Pei^{71,58}, M. Pelizaeus³, H. P. Peng^{71,58}, Y. Y. Peng^{38,j,k}, K. Peters^{13,d}, J. L. Ping⁴¹, R. G. Ping^{1,63}, S. Plura³⁵, V. Prasad³³, F. Z. Qi¹, H. Qi^{71,58}, H. R. Qi⁶¹, M. Qi⁴², T. Y. Qi^{12,f}, S. Qian^{1,58}, W. B. Qian⁶³, C. F. Qiao⁶³, J. J. Qin⁷², L. Q. Qin¹⁴, X. S. Qin⁵⁰, Z. H. Qin^{1,58}, J. F. Qiu¹, S. Q. Qu⁶¹, C. F. Redmer³⁵, K. J. Ren³⁹, A. Rivetti^{74C}, M. Rolo^{74C}, G. Rong^{1,63}, Ch. Rosner¹⁸, S. N. Ruan⁴³, N. Salone⁴⁴, A. Sarantsev^{36,c}, Y. Schelhaas³⁵, K. Schoenning⁷⁵, M. Scodreggio^{29A,29B}, K. Y. Shan^{12,f}, W. Shan²⁴, X. Y. Shan^{71,58}, J. F. Shangguan⁵⁵, L. G. Shao^{1,63}, M. Shao^{71,58}, C. P. Shen^{12,f}, H. F. Shen^{1,63}, W. H. Shen⁶³, X. Y. Shen^{1,63}, B. A. Shi⁶³, H. C. Shi^{71,58}, J. L. Shi¹², J. Y. Shi¹, Q. Q. Shi⁵⁵, R. S. Shi^{1,63}, X. Shi^{1,58}, J. J. Song¹⁹, T. Z. Song⁵⁹, W. M. Song^{34,1}, Y. J. Song¹², Y. X. Song^{46,g}, S. Sosio^{74A,74C}, S. Spataro^{74A,74C}, F. Stieler³⁵, Y. J. Su⁶³, G. B. Sun⁷⁶, G. X. Sun¹, H. Sun⁶³, H. K. Sun¹, J. F. Sun¹⁹, K. Sun⁶¹, L. Sun⁷⁶, S. S. Sun^{1,63}, T. Sun^{51,e}, W. Y. Sun³⁴, Y. Sun⁹, Y. J. Sun^{71,58}, Y. Z. Sun¹, Z. T. Sun⁵⁰, Y. X. Tan^{71,58}, C. J. Tang⁵⁴, G. Y. Tang¹, J. Tang⁵⁹, Y. A. Tang⁷⁶, L. Y. Tao⁷², Q. T. Tao^{25,h}, M. Tat⁶⁹, J. X. Teng^{71,58}, V. Thoren⁷⁵, W. H. Tian⁵², W. H. Tian⁵⁹, Y. Tian^{31,63}, Z. F. Tian⁷⁶, I. Uman^{62B}, Y. Wan⁵⁵, S. J. Wang⁵⁰, B. Wang¹, B. L. Wang⁶³, Bo Wang^{71,58}, C. W. Wang⁴², D. Y. Wang^{46,g}, F. Wang⁷², H. J. Wang^{38,j,k}, J. P. Wang⁵⁰, K. Wang^{1,58}, L. L. Wang¹, M. Wang⁵⁰, Meng Wang^{1,63}, N. Y. Wang⁶³, S. Wang^{38,j,k}, S. Wang^{12,f}, T. Wang^{12,f}, T. J. Wang⁴³, W. Wang⁵⁹, W. Wang⁷², W. P. Wang^{71,58}, X. Wang^{46,g}, X. F. Wang^{38,j,k}, X. J. Wang³⁹,

X. L. Wang^{12,f}, Y. Wang⁶¹, Y. D. Wang⁴⁵, Y. F. Wang^{1,58,63}, Y. L. Wang¹⁹, Y. N. Wang⁴⁵, Y. Q. Wang¹, Yaqian Wang^{17,1}, Yi Wang⁶¹, Z. Wang^{1,58}, Z. L. Wang⁷², Z. Y. Wang^{1,63}, Ziyi Wang⁶³, D. Wei⁷⁰, D. H. Wei¹⁴, F. Weidner⁶⁸, S. P. Wen¹, C. W. Wenzel³, U. Wiedner³, G. Wilkinson⁶⁹, M. Wolke⁷⁵, L. Wollenberg³, C. Wu³⁹, J. F. Wu^{1,8}, L. H. Wu¹, L. J. Wu^{1,63}, X. Wu^{12,f}, X. H. Wu³⁴, Y. Wu⁷¹, Y. H. Wu⁵⁵, Y. J. Wu³¹, Z. Wu^{1,58}, L. Xia^{71,58}, X. M. Xian³⁹, T. Xiang^{46,g}, D. Xiao^{38,j,k}, G. Y. Xiao⁴², S. Y. Xiao¹, Y. L. Xiao^{12,f}, Z. J. Xiao⁴¹, C. Xie⁴², X. H. Xie^{46,g}, Y. Xie⁵⁰, Y. G. Xie^{1,58}, Y. H. Xie⁶, Z. P. Xie^{71,58}, T. Y. Xing^{1,63}, C. F. Xu^{1,63}, C. J. Xu⁵⁹, G. F. Xu¹, H. Y. Xu⁶⁶, Q. J. Xu¹⁶, Q. N. Xu³⁰, W. Xu¹, W. L. Xu⁶⁶, X. P. Xu⁵⁵, Y. C. Xu⁷⁸, Z. P. Xu⁴², Z. S. Xu⁶³, F. Yan^{12,f}, L. Yan^{12,f}, W. B. Yan^{71,58}, W. C. Yan⁸¹, X. Q. Yan¹, H. J. Yang^{51,e}, H. L. Yang³⁴, H. X. Yang¹, Tao Yang¹, Y. Yang^{12,f}, Y. F. Yang⁴³, Y. X. Yang^{1,63}, Yifan Yang^{1,63}, Z. W. Yang^{38,j,k}, Z. P. Yao⁵⁰, M. Ye^{1,58}, M. H. Ye⁸, J. H. Yin¹, Z. Y. You⁵⁹, B. X. Yu^{1,58,63}, C. X. Yu⁴³, G. Yu^{1,63}, J. S. Yu^{25,h}, T. Yu⁷², X. D. Yu^{46,g}, C. Z. Yuan^{1,63}, L. Yuan², S. C. Yuan¹, X. Q. Yuan¹, Y. Yuan^{1,63}, Z. Y. Yuan⁵⁹, C. X. Yue³⁹, A. A. Zafar⁷³, F. R. Zeng⁵⁰, S. H. Zeng⁷², X. Zeng^{12,f}, Y. Zeng^{25,h}, Y. J. Zeng^{1,63}, X. Y. Zhai³⁴, Y. C. Zhai⁵⁰, Y. H. Zhan⁵⁹, A. Q. Zhang^{1,63}, B. L. Zhang^{1,63}, B. X. Zhang¹, D. H. Zhang⁴³, G. Y. Zhang¹⁹, H. Zhang⁷¹, H. C. Zhang^{1,58,63}, H. H. Zhang⁵⁹, H. H. Zhang³⁴, H. Q. Zhang^{1,58,63}, H. Y. Zhang^{1,58}, J. Zhang⁵⁹, J. Zhang⁸¹, J. J. Zhang⁵², J. L. Zhang²⁰, J. Q. Zhang⁴¹, J. W. Zhang^{1,58,63}, J. X. Zhang^{38,j,k}, J. Y. Zhang¹, J. Z. Zhang^{1,63}, Jianyu Zhang⁶³, L. M. Zhang⁶¹, L. Q. Zhang⁵⁹, Lei Zhang⁴², P. Zhang^{1,63}, Q. Y. Zhang^{39,81}, Shuihan Zhang^{1,63}, Shulei Zhang^{25,h}, X. D. Zhang⁴⁵, X. M. Zhang¹, X. Y. Zhang⁵⁰, Y. Zhang⁶⁹, Y. Zhang⁷², Y. T. Zhang⁸¹, Y. H. Zhang^{1,58}, Yan Zhang^{71,58}, Yao Zhang¹, Z. D. Zhang¹, Z. H. Zhang¹, Z. L. Zhang³⁴, Z. Y. Zhang⁴³, Z. Y. Zhang⁷⁶, G. Zhao¹, J. Y. Zhao^{1,63}, J. Z. Zhao^{1,58}, Lei Zhao^{71,58}, Ling Zhao¹, M. G. Zhao⁴³, R. P. Zhao⁶³, S. J. Zhao⁸¹, Y. B. Zhao^{1,58}, Y. X. Zhao^{31,63}, Z. G. Zhao^{71,58}, A. Zhemchugov^{36,a}, B. Zheng⁷², J. P. Zheng^{1,58}, W. J. Zheng^{1,63}, Y. H. Zheng⁶³, B. Zhong⁴¹, X. Zhong⁵⁹, H. Zhou⁵⁰, L. P. Zhou^{1,63}, X. Zhou⁷⁶, X. K. Zhou⁶, X. R. Zhou^{71,58}, X. Y. Zhou³⁹, Y. Z. Zhou^{12,f}, J. Zhu⁴³, K. Zhu¹, K. J. Zhu^{1,58,63}, L. Zhu³⁴, L. X. Zhu⁶³, S. H. Zhu⁷⁰, S. Q. Zhu⁴², T. J. Zhu^{12,f}, W. J. Zhu^{12,f}, Y. C. Zhu^{71,58}, Z. A. Zhu^{1,63}, J. H. Zou¹, J. Zu^{71,58}

(BESIII Collaboration)

¹ Institute of High Energy Physics, Beijing 100049, People's Republic of China

² Beihang University, Beijing 100191, People's Republic of China

³ Bochum Ruhr-University, D-44780 Bochum, Germany

⁴ Budker Institute of Nuclear Physics SB RAS (BINP), Novosibirsk 630090, Russia

⁵ Carnegie Mellon University, Pittsburgh, Pennsylvania 15213, USA

⁶ Central China Normal University, Wuhan 430079, People's Republic of China

⁷ Central South University, Changsha 410083, People's Republic of China

⁸ China Center of Advanced Science and Technology, Beijing 100190, People's Republic of China

⁹ China University of Geosciences, Wuhan 430074, People's Republic of China

¹⁰ Chung-Ang University, Seoul, 06974, Republic of Korea

¹¹ COMSATS University Islamabad, Lahore Campus, Defence Road, Off Raiwind Road, 54000 Lahore, Pakistan

¹² Fudan University, Shanghai 200433, People's Republic of China

¹³ GSI Helmholtzcentre for Heavy Ion Research GmbH, D-64291 Darmstadt, Germany

¹⁴ Guangxi Normal University, Guilin 541004, People's Republic of China

¹⁵ Guangxi University, Nanning 530004, People's Republic of China

¹⁶ Hangzhou Normal University, Hangzhou 310036, People's Republic of China

¹⁷ Hebei University, Baoding 071002, People's Republic of China

¹⁸ Helmholtz Institute Mainz, Staudinger Weg 18, D-55099 Mainz, Germany

¹⁹ Henan Normal University, Xinxiang 453007, People's Republic of China

²⁰ Henan University, Kaifeng 475004, People's Republic of China

²¹ Henan University of Science and Technology, Luoyang 471003, People's Republic of China

²² Henan University of Technology, Zhengzhou 450001, People's Republic of China

²³ Huangshan College, Huangshan 245000, People's Republic of China

²⁴ Hunan Normal University, Changsha 410081, People's Republic of China

²⁵ Hunan University, Changsha 410082, People's Republic of China

²⁶ Indian Institute of Technology Madras, Chennai 600036, India

²⁷ Indiana University, Bloomington, Indiana 47405, USA

²⁸ INFN Laboratori Nazionali di Frascati, (A)INFN Laboratori Nazionali di Frascati, I-00044, Frascati, Italy; (B)INFN Sezione di Perugia, I-06100, Perugia, Italy; (C)University of Perugia, I-06100, Perugia, Italy

²⁹ INFN Sezione di Ferrara, (A)INFN Sezione di Ferrara, I-44122, Ferrara, Italy; (B)University of Ferrara, I-44122, Ferrara, Italy

- ³⁰ Inner Mongolia University, Hohhot 010021, People's Republic of China
- ³¹ Institute of Modern Physics, Lanzhou 730000, People's Republic of China
- ³² Institute of Physics and Technology, Peace Avenue 54B, Ulaanbaatar 13330, Mongolia
- ³³ Instituto de Alta Investigación, Universidad de Tarapacá, Casilla 7D, Arica 1000000, Chile
- ³⁴ Jilin University, Changchun 130012, People's Republic of China
- ³⁵ Johannes Gutenberg University of Mainz, Johann-Joachim-Becher-Weg 45, D-55099 Mainz, Germany
- ³⁶ Joint Institute for Nuclear Research, 141980 Dubna, Moscow region, Russia
- ³⁷ Justus-Liebig-Universitaet Giessen, II. Physikalisches Institut, Heinrich-Buff-Ring 16, D-35392 Giessen, Germany
- ³⁸ Lanzhou University, Lanzhou 730000, People's Republic of China
- ³⁹ Liaoning Normal University, Dalian 116029, People's Republic of China
- ⁴⁰ Liaoning University, Shenyang 110036, People's Republic of China
- ⁴¹ Nanjing Normal University, Nanjing 210023, People's Republic of China
- ⁴² Nanjing University, Nanjing 210093, People's Republic of China
- ⁴³ Nankai University, Tianjin 300071, People's Republic of China
- ⁴⁴ National Centre for Nuclear Research, Warsaw 02-093, Poland
- ⁴⁵ North China Electric Power University, Beijing 102206, People's Republic of China
- ⁴⁶ Peking University, Beijing 100871, People's Republic of China
- ⁴⁷ Qufu Normal University, Qufu 273165, People's Republic of China
- ⁴⁸ Renmin University of China, Beijing 100872, People's Republic of China
- ⁴⁹ Shandong Normal University, Jinan 250014, People's Republic of China
- ⁵⁰ Shandong University, Jinan 250100, People's Republic of China
- ⁵¹ Shanghai Jiao Tong University, Shanghai 200240, People's Republic of China
- ⁵² Shanxi Normal University, Linfen 041004, People's Republic of China
- ⁵³ Shanxi University, Taiyuan 030006, People's Republic of China
- ⁵⁴ Sichuan University, Chengdu 610064, People's Republic of China
- ⁵⁵ Soochow University, Suzhou 215006, People's Republic of China
- ⁵⁶ South China Normal University, Guangzhou 510006, People's Republic of China
- ⁵⁷ Southeast University, Nanjing 211100, People's Republic of China
- ⁵⁸ State Key Laboratory of Particle Detection and Electronics, Beijing 100049, Hefei 230026, People's Republic of China
- ⁵⁹ Sun Yat-Sen University, Guangzhou 510275, People's Republic of China
- ⁶⁰ Suranaree University of Technology, University Avenue 111, Nakhon Ratchasima 30000, Thailand
- ⁶¹ Tsinghua University, Beijing 100084, People's Republic of China
- ⁶² Turkish Accelerator Center Particle Factory Group, (A)Istinye University, 34010, Istanbul, Turkey; (B)Near East University, Nicosia, North Cyprus, 99138, Mersin 10, Turkey
- ⁶³ University of Chinese Academy of Sciences, Beijing 100049, People's Republic of China
- ⁶⁴ University of Groningen, NL-9747 AA Groningen, The Netherlands
- ⁶⁵ University of Hawaii, Honolulu, Hawaii 96822, USA
- ⁶⁶ University of Jinan, Jinan 250022, People's Republic of China
- ⁶⁷ University of Manchester, Oxford Road, Manchester, M13 9PL, United Kingdom
- ⁶⁸ University of Muenster, Wilhelm-Klemm-Strasse 9, 48149 Muenster, Germany
- ⁶⁹ University of Oxford, Keble Road, Oxford OX13RH, United Kingdom
- ⁷⁰ University of Science and Technology Liaoning, Anshan 114051, People's Republic of China
- ⁷¹ University of Science and Technology of China, Hefei 230026, People's Republic of China
- ⁷² University of South China, Hengyang 421001, People's Republic of China
- ⁷³ University of the Punjab, Lahore-54590, Pakistan
- ⁷⁴ University of Turin and INFN, (A)University of Turin, I-10125, Turin, Italy; (B)University of Eastern Piedmont, I-15121, Alessandria, Italy; (C)INFN, I-10125, Turin, Italy
- ⁷⁵ Uppsala University, Box 516, SE-75120 Uppsala, Sweden
- ⁷⁶ Wuhan University, Wuhan 430072, People's Republic of China
- ⁷⁷ Xinyang Normal University, Xinyang 464000, People's Republic of China
- ⁷⁸ Yantai University, Yantai 264005, People's Republic of China
- ⁷⁹ Yunnan University, Kunming 650500, People's Republic of China
- ⁸⁰ Zhejiang University, Hangzhou 310027, People's Republic of China

⁸¹ Zhengzhou University, Zhengzhou 450001, People's Republic of China

^a Also at the Moscow Institute of Physics and Technology, Moscow 141700, Russia

^b Also at the Novosibirsk State University, Novosibirsk, 630090, Russia

^c Also at the NRC "Kurchatov Institute", PNPI, 188300, Gatchina, Russia

^d Also at Goethe University Frankfurt, 60323 Frankfurt am Main, Germany

^e Also at Key Laboratory for Particle Physics, Astrophysics and Cosmology, Ministry of Education; Shanghai Key Laboratory for Particle Physics and Cosmology; Institute of Nuclear and Particle Physics, Shanghai 200240, People's Republic of China

^f Also at Key Laboratory of Nuclear Physics and Ion-beam Application (MOE) and Institute of Modern Physics, Fudan University, Shanghai 200443, People's Republic of China

^g Also at State Key Laboratory of Nuclear Physics and Technology, Peking University, Beijing 100871, People's Republic of China

^h Also at School of Physics and Electronics, Hunan University, Changsha 410082, China

ⁱ Also at Guangdong Provincial Key Laboratory of Nuclear Science, Institute of Quantum Matter, South China Normal University, Guangzhou 510006, China

^j Also at MOE Frontiers Science Center for Rare Isotopes, Lanzhou University, Lanzhou 730000, People's Republic of China

^k Also at Lanzhou Center for Theoretical Physics, Lanzhou University, Lanzhou 730000, People's Republic of China

^l Also at the Department of Mathematical Sciences, IBA, Karachi 75270, Pakistan

(Dated: February 14, 2025)

Using a data sample corresponding to an integrated luminosity of 10.9 fb^{-1} collected at center-of-mass energies from 4.16 to 4.34 GeV with the BESIII detector, we search for the decay $\chi_{c1}(3872) \rightarrow \pi^+\pi^-\chi_{c1}$ in the radiative production $e^+e^- \rightarrow \gamma\chi_{c1}(3872)$. No significant signal is observed, and the ratio for the branching fraction of $\chi_{c1}(3872) \rightarrow \pi^+\pi^-\chi_{c1}$ to $\chi_{c1}(3872) \rightarrow \pi^+\pi^-J/\psi$ is measured as $\mathcal{R} \equiv \frac{\mathcal{B}[\chi_{c1}(3872) \rightarrow \pi^+\pi^-\chi_{c1}]}{\mathcal{B}[\chi_{c1}(3872) \rightarrow \pi^+\pi^-J/\psi]} < 0.18$ at 90% confidence level. An upper limit on the product of the cross section $\sigma[e^+e^- \rightarrow \gamma\chi_{c1}(3872)]$ and the branching fraction $\mathcal{B}[\chi_{c1}(3872) \rightarrow \pi^+\pi^-\chi_{c1}]$ at each center-of-mass energy is also given. These measurements favor the non-conventional charmonium nature of the $\chi_{c1}(3872)$ state.

The $\chi_{c1}(3872)$ charmonium-like state was first discovered in 2003 by the Belle experiment in the decay $B \rightarrow K\chi_{c1}(3872) \rightarrow K\pi^+\pi^-J/\psi$ [1]. It was then observed by many experiments in various production and decay modes [2, 3]. The main features of the $\chi_{c1}(3872)$ are the following: it is a narrow state, $\Gamma = 1.19 \pm 0.21 \text{ MeV}$; its mass is very close to the $D^0\bar{D}^{*0}$ threshold, with an error of $0.18 \text{ MeV}/c^2$; and it has quantum numbers $J^{PC} = 1^{++}$. Also, there is an obvious isospin-violation effect in its decays, e.g. the decay $\chi_{c1}(3872) \rightarrow \pi^+\pi^-J/\psi$ has been found to proceed predominantly via $\rho J/\psi$ [2]. The experimentally well-established decay channels of the $\chi_{c1}(3872)$ include $\chi_{c1}(3872) \rightarrow \pi^+\pi^-J/\psi$ [1, 4, 5], $D^0\bar{D}^{*0}$ [6, 7], $\gamma J/\psi$ [7, 8], $\pi^0\chi_{c1}$ [9], and $\omega J/\psi$ [10, 11]. Theoretical interpretations of the nature of the $\chi_{c1}(3872)$ state include a tetraquark state [12], the $\chi_{c1}(2P)$ charmonium state [13], and a $D^0\bar{D}^{*0}$ molecule state [14, 15], without a definitive conclusion. Therefore, more detailed studies of $\chi_{c1}(3872)$ from both experimental and theoretical sides are necessary for an in-depth knowledge of the $\chi_{c1}(3872)$ internal structure.

Unlike $\chi_{c1}(3872) \rightarrow \omega J/\psi$, the decay $\chi_{c1}(3872) \rightarrow \pi^0\chi_{c1}$ is isospin-violating and presumed to be highly suppressed. However, the BESIII experiment has observed the decay $\chi_{c1}(3872) \rightarrow \pi^0\chi_{c1}$, with a relative branching fraction ratio $\frac{\mathcal{B}[\chi_{c1}(3872) \rightarrow \pi^0\chi_{c1}]}{\mathcal{B}[\chi_{c1}(3872) \rightarrow \pi^+\pi^-J/\psi]} = 0.88^{+0.33}_{-0.27} \pm 0.10$ [9]. Taking into account $\frac{\mathcal{B}[\chi_{c1}(3872) \rightarrow \omega J/\psi]}{\mathcal{B}[\chi_{c1}(3872) \rightarrow \pi^+\pi^-J/\psi]} = 1.6^{+0.4}_{-0.3} \pm 0.2$ [11], the branching fraction $\mathcal{B}[\chi_{c1}(3872) \rightarrow \pi^0\chi_{c1}]$ has a size similar to $\mathcal{B}[\chi_{c1}(3872) \rightarrow \omega J/\psi]$. This unexpectedly large isospin-

violation indicates that $\chi_{c1}(3872)$ may not be a conventional charmonium.

If the $\chi_{c1}(3872)$ is the $\chi_{c1}(2P)$ charmonium state, isospin-conserving decays, such as $\chi_{c1}(3872) \rightarrow \pi^+\pi^-\chi_{c1}$, are expected to dominate. Theoretical calculations show that the one-pion transition is significantly suppressed with respect to the di-pion transition, with $\frac{\Gamma(2^3P_1 \rightarrow \chi_{c1}\pi^0)}{\Gamma(2^3P_1 \rightarrow \chi_{c1}\pi^+\pi^-)} \approx 0.04$ [16]. However, the one-pion transition rate could be enhanced assuming the $\chi_{c1}(3872)$ is a shallow bound state of a \bar{D}^0D^{*0} pair [17]. Therefore experimental studies of the decay $\chi_{c1}(3872) \rightarrow \pi^+\pi^-\chi_{c1}$ help to discriminate theoretical interpretations for the nature of the $\chi_{c1}(3872)$.

In this article, we report on the search for the process $e^+e^- \rightarrow \gamma\chi_{c1}(3872) \rightarrow \gamma(\pi^+\pi^-\chi_{c1})$. The χ_{c1} candidate is reconstructed via its decay to $\gamma J/\psi$, with $J/\psi \rightarrow \ell^+\ell^-$ ($\ell = e$ or μ). Due to the relatively low momenta, pions may not be fully detected. To increase the signal yield, events with either one or two detected pions are used for signal reconstruction. The data sample is taken with the BESIII detector [18] at fifteen center-of-mass (c.m.) energies ranging from $\sqrt{s} = 4.16$ to 4.34 GeV [19], corresponding to an integrated luminosity of 10.9 fb^{-1} [20].

The BESIII detector [18] records symmetric e^+e^- collisions provided by the BEPCII storage ring [21] in the c.m. energy region from 2.0 to 4.95 GeV, with a peak luminosity of $1 \times 10^{33} \text{ cm}^{-2}\text{s}^{-1}$ achieved at $\sqrt{s} = 3.773 \text{ GeV}$. The cylindrical core of the BESIII detector covers 93% of the full solid angle and consists of a helium-based multilayer drift cham-

ber (MDC), a plastic scintillator time-of-flight system (TOF), and a CsI(Tl) electromagnetic calorimeter (EMC), which are all enclosed in a superconducting solenoidal magnet providing a 1.0 T magnetic field. The solenoid is supported by an octagonal flux-return yoke with resistive plate counter muon identification modules interleaved with steel [22]. The charged-particle momentum resolution at 1 GeV/c is 0.5%, and the dE/dx resolution is 6% for electrons from Bhabha scattering. The EMC measures photon energies with a resolution of 2.5% (5%) at 1 GeV in the barrel (end cap) region. The time resolution in the TOF barrel region is 68 ps, while that in the end cap region was 110 ps. The end cap TOF system was upgraded in 2015 using multigap resistive plate chamber technology, providing a time resolution of 60 ps [23]. About 83% of the data used here benefits from this upgrade.

Simulated data samples produced with a GEANT4-based [24] Monte Carlo (MC) simulation software package, which includes the BESIII detector response and geometric description, are used to optimize the event selection criteria, determine the detection efficiency, and estimate the backgrounds. For the signal process, we generate 100,000 $e^+e^- \rightarrow \gamma\chi_{c1}(3872)$ events at each c.m. energy, assuming an E1 radiative transition process which has been confirmed by BESIII data [5]. The $\chi_{c1}(3872) \rightarrow \pi^+\pi^-\chi_{c1}$ decay is described with the phase-space model in EVTGEN [25]. Initial-state-radiation (ISR) is simulated with KKMC [26], by incorporating the \sqrt{s} -dependent production cross section of $e^+e^- \rightarrow \gamma\chi_{c1}(3872)$ into the program [11]. The maximum ISR photon energy is set according to the production threshold of the $\gamma\chi_{c1}(3872)$ system. Final-state-radiation is simulated with the PHOTOS package [27].

The background contributions are investigated using an inclusive MC sample, which includes the production of open-charm processes, the ISR production of vector charmonium(-like) states, and the continuum processes incorporated in KKMC. All particle decays are modelled with the EVTGEN [25] using branching fractions taken from the Particle Data Group (PDG) [2] when available, and otherwise modelled with LUNDCHARM [28]. The equivalent luminosity of the inclusive MC sample is 40 times that of data at $\sqrt{s} = 4.178$ GeV, and is of equal size to data at other c.m. energies. A generic event-type analysis tool, TopoAna [29], is employed to study the backgrounds.

Charged tracks are required to be within a polar angle range of $|\cos\theta| < 0.93$, where θ is defined with respect to the z -axis (the symmetry axis of the MDC). For each charged track, the distance of the closest approach to the interaction point (IP) must be less than 10 cm along the z -axis, and less than 1 cm in the transverse plane. The pions from the $\chi_{c1}(3872)$ decay and the leptons from the J/ψ decay are kinematically well-separated. Thus, charged tracks with momenta greater than 1.0 GeV/c in the laboratory frame are taken as lepton candidates, while those with momenta less than 0.3 GeV/c are taken as pion candidates due to limited phase space. The energy deposition in the EMC of a lepton candidate is used to separate e from μ . Both μ candidates are required to have deposited energies less than 0.4 GeV, while both e candidates are required to have deposited energies greater than 1.1 GeV.

Photon candidates are identified using showers in the EMC. The deposited energy of each shower must be more than 25 MeV in the barrel region ($|\cos\theta| < 0.80$) and more than 50 MeV in the end cap region ($0.86 < |\cos\theta| < 0.92$). To exclude showers that originate from charged tracks, the angle subtended by the EMC shower and the position of the closest charged track at the EMC must be greater than 10 degrees as measured from the IP. To suppress electronic noise and showers unrelated to the event, the difference between the EMC time of a shower and the event start time is required to be within [0, 700] ns. At least two good photon candidates are required in each event.

For an event with one soft pion undetected, the number of charged tracks ($\pi^\pm\ell^+\ell^-$) in the event is required to be three (referred to as a 3-track event). The four-momentum of the missing pion is obtained from four-momentum conservation and the initial beam kinematics. A one-constraint (1C) kinematic fit is then applied to each candidate event, where the mass of the missing particle is constrained to the pion mass. If there is more than one combination within an event due to additional photon candidates, we retain the two photons corresponding to the minimum χ^2 from the 1C kinematic fit. To further distinguish the radiative photon in $e^+e^- \rightarrow \gamma_{\text{rad}}\chi_{c1}(3872)$ and the photon from χ_{c1} decay, an extra constraint is added to constrain the $\gamma\ell^+\ell^-$ invariant mass to the χ_{c1} mass. The combination with the minimum χ^2 from the 2C kinematic fit is assigned as the correct combination, and events with $\chi^2_{2C} < 16$ are selected.

There are background events from the $e^+e^- \rightarrow \gamma_{\text{ISR}}\psi(2S) \rightarrow \gamma_{\text{ISR}}\pi^+\pi^-J/\psi$ process, together with one fake photon candidate. To remove such events, we require $\frac{E_\gamma^H - E_\gamma^L}{E_\gamma^H + E_\gamma^L} < 0.25$, where E_γ^H and E_γ^L are the energies of the higher and lower energy photons in an event, respectively. This criterion is very effective at rejecting background while retaining high signal efficiency. To reject γ conversion ($\gamma \rightarrow e^+e^-$) background events, where the converted electrons are misidentified as pions, particle identification (PID) for charged pion, combining measurements of the specific ionization energy loss in the MDC and the flight time in the TOF to form likelihoods $\mathcal{L}(h)$ ($h = p, K, \pi$) for each hadron h hypothesis, is performed. Tracks with momentum less than 0.3 GeV/c must satisfy $\mathcal{L}(\pi) > \mathcal{L}(e)$. Background events from the $e^+e^- \rightarrow \eta J/\psi \rightarrow \pi^+\pi^-\pi^0 J/\psi$ process are effectively vetoed by requiring $M(\gamma\gamma\pi^+\pi^-) > 0.6$ GeV/c².

For events with both pions detected, the total number of charged tracks ($\pi^+\pi^-\ell^+\ell^-$) must be at least four (referred to as 4-track events), with exactly two oppositely-charged leptons, and at least two oppositely-charged pions. A four-constraint (4C) kinematic fit imposing four-momentum conservation is performed to each event. If there is more than one combination due to extra pion or extra photon candidates, we retain the one with the minimum χ^2 value from the 4C kinematic fit. An extra constraint is added to constrain $\gamma\ell^+\ell^-$ to the χ_{c1} mass, to distinguish the photon from the χ_{c1} decay and the radiative photon associated with $\chi_{c1}(3872)$ production. The combination with the minimum χ^2 from this 5C kinematic fit is assigned as the correct one. Events with

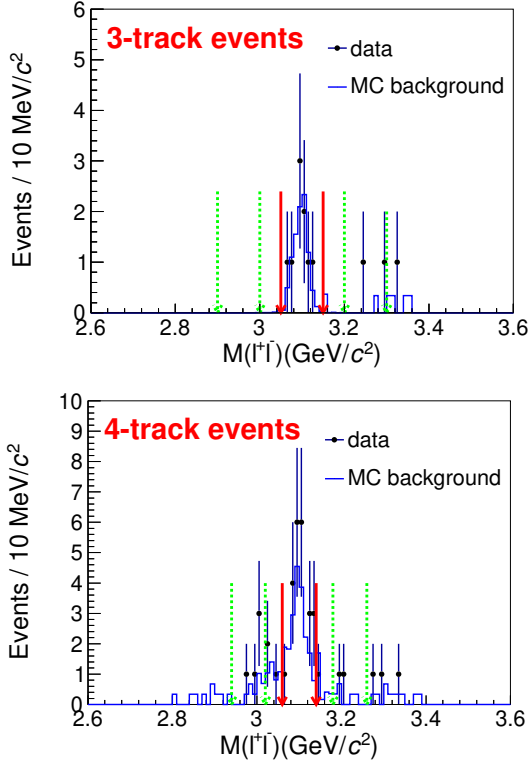


FIG. 1. The distribution of $M(\ell^+\ell^-)$ for data and MC background for 3-track events (top) and 4-track events (bottom). The dots with error bars are the full data. The blue histogram represents the MC background, which come from the contributions of $\eta'J/\psi$, $\pi^+\pi^-\psi(3823)$, $\gamma_{\text{ISR}}\psi'$ and continue background. The area between the red solid arrows is the signal area of J/ψ , and the area between the green dotted arrows is the sideband area of J/ψ .

$\chi^2_{5C} < 80$ are kept for further analysis.

There are $\psi(2S)$ background events coming from $e^+e^- \rightarrow \pi^+\pi^-\psi(2S)$ with $\psi(2S) \rightarrow \gamma\chi_{c1}/\pi^0\pi^0 J/\psi$, and $e^+e^- \rightarrow \gamma_{\text{ISR}}\psi(2S)/\eta\psi(2S)$ with $\psi(2S) \rightarrow \pi^+\pi^- J/\psi$. These background events are effectively vetoed by requiring the recoil mass of the $\pi^+\pi^-$ system to satisfy $M^{\text{recoil}}(\pi^+\pi^-) = \sqrt{(P_{e^+e^-} - P_{\pi^+\pi^-})^2} > 3.704 \text{ GeV}/c^2$, and the invariant mass $M(\pi^+\pi^- J/\psi) < 3.660 \text{ GeV}/c^2$. Here $P_{e^+e^-}$ and $P_{\pi^+\pi^-}$ are the four-momenta of the initial colliding beams and the $\pi^+\pi^-$ pair, respectively. The γ -conversion background events are effectively eliminated by requiring the opening angle of the pion pair to satisfy $\cos\theta_{\pi^+\pi^-} < 0.98$. Background events from the $e^+e^- \rightarrow \eta J/\psi \rightarrow \pi^+\pi^-\pi^0 J/\psi$ process are rejected by requiring $M(\gamma\pi^+\pi^-) > 0.59 \text{ GeV}/c^2$.

The $M(\ell^+\ell^-)$ mass distribution after performing the above selections is shown in Fig. 1. To select signal candidates that contain a J/ψ resonance, we define $[3.05, 3.15] \text{ GeV}/c^2$ (for 3-track events), and $[3.06, 3.14] \text{ GeV}/c^2$ (for 4-track events) as the J/ψ mass windows. The non- J/ψ background contribution is estimated by the events in the J/ψ mass sideband regions, which are defined as $[2.90, 3.00] \text{ GeV}/c^2$ or $[3.20, 3.30] \text{ GeV}/c^2$ (for 3-track events), and $[2.94, 3.02] \text{ GeV}/c^2$ or $[3.18, 3.26] \text{ GeV}/c^2$ (for 4-track events), respectively.

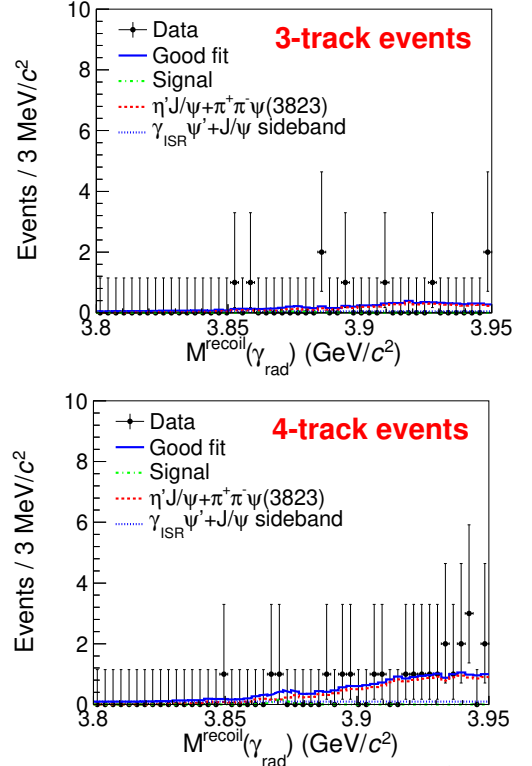


FIG. 2. Result of the simultaneous fit to the $M^{\text{recoil}}(\gamma_{\text{rad}})$ distributions for 3-track events (top) and 4-track events (bottom). The dots with error bars are the full data, the blue solid curves represent the total fit, the green dash-dotted curves are the signal contribution, and the blue dotted curves and red dashed curves are the background contributions.

Figure 2 shows the recoil mass distribution of the radiative photon $M^{\text{recoil}}(\gamma_{\text{rad}}) = \sqrt{(P_{e^+e^-} - P_{\gamma_{\text{rad}}})^2}$ from the full data set after imposing the above requirements. Here $P_{\gamma_{\text{rad}}}$ is the four-momenta of the radiative photon γ_{rad} . The background level is very low, and no obvious $\chi_{c1}(3872)$ signal is observed. Possible remaining background contributions mainly come from the $e^+e^- \rightarrow \eta' J/\psi \rightarrow \pi^+\pi^-\eta J/\psi$ and $e^+e^- \rightarrow \pi^+\pi^-\psi_2(3823) \rightarrow \gamma\pi^+\pi^-\chi_{c1}$ processes. These background contributions have been well-studied by BESIII [30, 31] and can be reliably simulated, as shown in Fig. 2. According to a study of the J/ψ mass sideband events and inclusive MC events, the non- J/ψ background and $\gamma_{\text{ISR}}\psi(2S)$ contributions are found to be small and only produce a flat distribution in the $\chi_{c1}(3872)$ signal region.

To extract the signal yield, a simultaneous unbinned maximum likelihood fit is performed to the $M^{\text{recoil}}(\gamma_{\text{rad}})$ distributions for the 3-track and 4-track events, as shown in Fig. 2. In the simultaneous fit, the ratio between the 3-track and 4-track events signal yields is fixed according to the detection efficiencies. The signal probability density function in the fit is represented by the MC-simulated $\chi_{c1}(3872)$ shape convolved with a Gaussian function, which accounts for the difference in mass resolution between data and MC simulation. The parameters of the $\chi_{c1}(3872)$ resonance in the simulation are taken from PDG [2], and those of the convolved Gaussian are

fixed according to a study of the $e^+e^- \rightarrow \gamma_{\text{ISR}}\psi(2S) \rightarrow \gamma_{\text{ISR}}\pi^+\pi^-J/\psi$ control sample. The background in the fit consists of two components. One is the simulated contribution from the $e^+e^- \rightarrow \eta'J/\psi$ and $e^+e^- \rightarrow \pi^+\pi^-\psi_2(3823)$ processes, which is normalized according to their measured cross sections [30, 31]. The other is a mass-independent term, which represents the contributions from the simulated $\gamma_{\text{ISR}}\psi(2S)$ background events and continuum background events estimated from J/ψ mass sideband data.

Since no obvious $\chi_{c1}(3872) \rightarrow \pi^+\pi^-\chi_{c1}$ signal is observed in the $M^{\text{recoil}}(\gamma_{\text{rad}})$ distributions, we estimate the upper limit (U.L.) for the produced number of $\chi_{c1}(3872) \rightarrow \pi^+\pi^-\chi_{c1}$ yield $N^{\text{sig}}(\pi^+\pi^-\chi_{c1})$ after efficiency correction. Based on the Bayesian method [32], the U.L. at a 90% confidence level (C.L.) is set to be $N^{\text{sig}}(\pi^+\pi^-\chi_{c1}) < 17.8$ by scanning the likelihood curve in the simultaneous fit with all the additive systematic uncertainties taken into account. To take into account the multiplicative systematic uncertainty, the likelihood curve is further convolved by a Gaussian with a width parameter equal to the total multiplicative systematic uncertainty, 13.2% ($\int_0^{+\infty} \mathcal{L}(N'_{\text{sig}}) e^{-\frac{(N_{\text{sig}} - N'_{\text{sig}})^2}{2(0.132N_{\text{sig}})^2}} dN'_{\text{sig}}$, where $N_{\text{sig}}^{(i)}$ is the signal yield, $\mathcal{L}(N'_{\text{sig}})$ is the likelihood curve). And the systematic uncertainties are discussed below. The most conservative estimate of U.L. after considering all systematic uncertainty is $N^{\text{sig}}(\pi^+\pi^-\chi_{c1}) < 18.5$ at a 90% C.L.

The relative branching ratio $\mathcal{R} \equiv \frac{\mathcal{B}[\chi_{c1}(3872) \rightarrow \pi^+\pi^-\chi_{c1}]}{\mathcal{B}[\chi_{c1}(3872) \rightarrow \pi^+\pi^-J/\psi]}$ is calculated as

$$\mathcal{R} = \frac{N^{\text{sig}}(\pi^+\pi^-\chi_{c1})\epsilon^{\text{ave}}(\pi^+\pi^-J/\psi)}{N^{\text{obs}}(\pi^+\pi^-J/\psi)\mathcal{B}(\chi_{c1} \rightarrow \gamma J/\psi)}, \quad (1)$$

where $N^{\text{obs}}(\pi^+\pi^-J/\psi) = 86.3^{+10.5}_{-9.8}$ is the signal yield of $\chi_{c1}(3872) \rightarrow \pi^+\pi^-J/\psi$ from the same data set, $\epsilon^{\text{ave}}(\pi^+\pi^-J/\psi) = 0.287$ is the weighted average efficiency of $\chi_{c1}(3872) \rightarrow \pi^+\pi^-J/\psi$ events [5], and $\mathcal{B}(\chi_{c1} \rightarrow \gamma J/\psi) = 0.343$ is the branching fraction of $\chi_{c1} \rightarrow \gamma J/\psi$ [2]. The U.L. for the ratio is determined to be $\mathcal{R} < 0.18$ at a 90% C.L.

The U.L. for the product of the cross section $\sigma[e^+e^- \rightarrow \gamma\chi_{c1}(3872)]$ and the branching fraction $\mathcal{B}[\chi_{c1}(3872) \rightarrow \pi^+\pi^-\chi_{c1}]$ is calculated as

$$\begin{aligned} \sigma[e^+e^- \rightarrow \gamma\chi_{c1}(3872)]\mathcal{B}[\chi_{c1}(3872) \rightarrow \pi^+\pi^-\chi_{c1}] \\ = \frac{N^{\text{U.L.}}}{\mathcal{L}_{\text{int}}(1+\delta)\epsilon_{\text{tot}}\mathcal{B}}, \quad (2) \end{aligned}$$

where \mathcal{L}_{int} is the integrated luminosity, $(1+\delta)$ is the radiative correction factor calculated by the KKMC program [26]. The symbol ϵ_{tot} is the sum of selection efficiencies for 3-track events and 4-track events, and $\mathcal{B} \equiv \mathcal{B}(\chi_{c1} \rightarrow \gamma J/\psi)\mathcal{B}(J/\psi \rightarrow \ell^+\ell^-)$ is a product of the corresponding branching fractions. $N^{\text{U.L.}}$ is the U.L. at a 90% C.L. for the signal yield at each c.m. energy, which is determined by counting the number of events in the $\chi_{c1}(3872)$ signal region [3.86, 3.88] GeV/ c^2 , due to the limited statistics. The

background has been subtracted, which is estimated by using the $\chi_{c1}(3872)$ sidebands [3.81, 3.84] GeV/ c^2 and [3.91, 3.94] GeV/ c^2 . The distributions of $M^{\text{recoil}}(\gamma_{\text{rad}})$ at each c.m. energy are shown in Appendix A Fig. 3. The $N^{\text{U.L.}}$ at each c.m. energy is calculated using a frequentist method with an unbounded profile likelihood treatment by assuming the numbers of observed events in the $\chi_{c1}(3872)$ signal and sideband regions follow a Poisson distribution [33]. Table I summarizes the results related to the $\sigma[e^+e^- \rightarrow \gamma\chi_{c1}(3872)]\mathcal{B}[\chi_{c1}(3872) \rightarrow \pi^+\pi^-\chi_{c1}]$ measurement.

For the \mathcal{R} measurement, many common systematic uncertainty sources cancel, including those arising from the luminosity, the lepton reconstruction efficiency, the kinematic fit, the branching fraction of $\mathcal{B}(J/\psi \rightarrow \ell^+\ell^-)$, and the ISR correction factor. The non-canceling systematic uncertainties consists of multiplicative and additive systematic uncertainties. The multiplicative are derived from the efficiencies for photon detection, pion tracking, PID, the branching fraction of $\chi_{c1} \rightarrow \gamma J/\psi$, the MC decay model, and those from $\chi_{c1}(3872) \rightarrow \pi^+\pi^-J/\psi$ channel. The uncertainty for photon detection is 1.0% per photon [34]. Since the efficiency for one photon does not cancel in \mathcal{R} , 1.0% is taken as the systematic uncertainty for photon detection. The pion pair in the search channel of $\chi_{c1}(3872) \rightarrow \pi^+\pi^-\chi_{c1}$ has a relatively low momentum compared to that of $\chi_{c1}(3872) \rightarrow \pi^+\pi^-J/\psi$. Thus the uncertainty of pion tracking does not cancel, and the uncertainty is estimated to be 1.0% per pion [35]. In the search channel, PID is applied for the pion candidate in 3-track event selection. The systematic uncertainty is assigned as 1.0% per pion. The systematic uncertainty related to the branching fraction $\mathcal{B}(\chi_{c1} \rightarrow \gamma J/\psi)$ is taken from PDG [2]. In the nominal analysis, the $\chi_{c1}(3872) \rightarrow \pi^+\pi^-\chi_{c1}$ signal MC events are generated using a phase-space model. Assuming the $\pi^+\pi^-$ system is dominated by a $\sigma(500)$ resonance, we generate alternative signal MC events for both S -wave and D -wave $\chi_{c1}(3872)$ decays, and the maximum difference to the nominal efficiency is taken as systematic uncertainty from an MC decay model. The systematic uncertainty from the $\chi_{c1}(3872) \rightarrow \pi^+\pi^-J/\psi$ channel is quoted from Ref. [5], including sources related to the pion tracking, signal parametrization, background shape, and the statistical uncertainty of the signal yield $N^{\text{sig}}(\pi^+\pi^-J/\psi)$.

Assuming that all of the multiplicative systematics are independent, the total multiplicative systematic uncertainty for the \mathcal{R} ratio measurement is obtained by adding all these individual uncertainties in quadrature, resulting in 13.2%, as shown in Table II.

Other additive uncertainties including backgrounds, the fit range and the signal shape affect $N^{\text{sig}}(\pi^+\pi^-\chi_{c1})$ directly. The uncertainty due to backgrounds in the $\chi_{c1}(3872) \rightarrow \pi^+\pi^-\chi_{c1}$ channel is investigated by floating the background contributions from $\eta'J/\psi$ and $\pi^+\pi^-\psi_2(3823)$ which were previously fixed based on MC studies. The uncertainty associated with the fit range is determined by varying the fit range within ± 10 MeV. The uncertainty due to the signal shape is considered by varying the resolution of the convolved Gaussian within $\pm 1\sigma$. The most conservative $N^{\text{sig}}(\pi^+\pi^-\chi_{c1})$ from the combined effects of these additive sources is taken

TABLE I. Summary of the integrated luminosities (\mathcal{L}_{int}) of data, the total efficiency of 3-track events and 4-track events (ϵ_{tot}), the ISR correction factor ($1+\delta$), the number of observed events, N_{obs} , the expected number of background events, N_{bkg} , in the $\chi_{c1}(3872)$ signal region for each sample, the obtained 90% C.L. upper limit for the $\chi_{c1}(3872)$ signal yields, $N^{\text{U.L.}}$, and the product $\sigma[e^+e^- \rightarrow \gamma\chi_{c1}(3872)]\mathcal{B}[\chi_{c1}(3872) \rightarrow \pi^+\pi^-\chi_{c1}]$ at each c.m. energy, denoted as $(\sigma\mathcal{B})^{\text{U.L.}}$, in pb. The multiplicative systematic uncertainties, denoted Δ in %, have been taken into account.

\sqrt{s} (GeV)	\mathcal{L}_{int} (pb $^{-1}$)	ϵ_{tot} (%)	$(1+\delta)$	N_{obs}	N_{bkg}	$N^{\text{U.L.}}$	$(\sigma\mathcal{B})^{\text{U.L.}}$	Δ (%)
4.158	408.2	32.6	0.78	0	0.3	1.8	0.50	5.3
4.178	3194.5	32.3	0.78	2	0.3	5.0	0.18	5.4
4.189	526.7	32.7	0.78	0	0.2	1.8	0.39	5.5
4.199	526.0	32.9	0.79	0	0.2	1.8	0.38	5.5
4.209	517.1	32.3	0.81	0	0.0	2.0	0.43	5.5
4.219	514.6	32.3	0.84	0	0.2	1.8	0.38	5.5
4.226	1056.4	32.8	0.86	0	0.3	1.7	0.17	5.4
4.236	530.3	32.0	0.89	0	0.1	1.9	0.37	5.4
4.244	538.1	31.6	0.92	0	0.1	1.9	0.37	5.4
4.258	828.4	30.9	0.97	0	0.0	2.0	0.25	5.4
4.267	531.1	30.0	1.00	0	0.0	2.0	0.40	5.4
4.278	175.7	28.8	1.05	0	0.0	2.0	1.24	5.6
4.288	502.4	28.3	1.09	0	0.1	1.9	0.43	5.5
4.312	501.1	26.2	1.19	0	0.0	2.0	0.44	5.5
4.338	504.9	23.9	1.30	0	0.0	2.0	0.43	5.5

TABLE II. Summary of the multiplicative systematic uncertainties (in %) for the \mathcal{R} measurement.

Source	3-track	4-track	Combined
Photon detection efficiency	1.0	1.0	1.0
Pion tracking efficiency	1.0	2.0	1.6
PID	1.0	...	0.5
$\mathcal{B}(\chi_{c1} \rightarrow \gamma J/\psi)$	3.0	3.0	3.0
MC decay model	2.8	2.8	2.8
$\chi_{c1}(3872) \rightarrow \pi^+\pi^- J/\psi$			12.4
Total			13.2

as the final result.

The systematic uncertainties in the $\sigma[e^+e^- \rightarrow \gamma\chi_{c1}(3872)]\mathcal{B}[\chi_{c1}(3872) \rightarrow \pi^+\pi^-\chi_{c1}]$ measurement include those from the luminosity, photon detection, tracking efficiency, PID, J/ψ mass window, kinematic fit, MC decay model, radiative correction and branching fraction. The luminosity is measured using large angle Bhabha events, with an uncertainty of 0.66% [20]. The systematic uncertainties related to the photon detection, PID, MC decay model and branching fraction of $\chi_{c1} \rightarrow \gamma J/\psi$ are the same as those in the \mathcal{R} measurement.

The uncertainty of tracking efficiency for the high-momentum leptons is 1.0% per track [36]. By requiring at least one pion to be detected, the pion detection efficiency is very high and the uncertainty is negligible. The uncertainty of $\mathcal{B}(J/\psi \rightarrow \ell^+\ell^-)$ is 0.6%, quoted from PDG [2]. The uncertainties caused by the J/ψ mass window are studied with a control sample of $e^+e^- \rightarrow \eta J/\psi$ events, with $\eta \rightarrow \pi^+\pi^-\pi^0$,

resulting in 0.55% and 0.04% for the 3-track events and 4-track events, respectively. A track helix parameter correction method is applied to the signal MC events [37] in the kinematic fit. The difference in efficiencies with and without the correction is assigned as the systematic uncertainty from the kinematic fit. To estimate the systematic uncertainty from radiative corrections (i.e., due to the uncertainty of the $e^+e^- \rightarrow \gamma\chi_{c1}(3872)$ cross section line shape [11]), we sample 300 line shapes using the resonance parameters ($M = 4200.6^{+7.9}_{-13.3} \pm 3.0$ MeV/ c^2 and $\Gamma = 115^{+38}_{-26} \pm 12$ MeV) within uncertainties, including their correlation, taken from Ref. [11]. A weight method [38] is used to get the distribution of $(1+\delta)\epsilon$, and the standard deviation of $(1+\delta)\epsilon$ is estimated as the systematic uncertainty from radiative correction.

Assuming that all the sources are independent, the total systematic uncertainty for $\sigma[e^+e^- \rightarrow \gamma\chi_{c1}(3872)]\mathcal{B}[\chi_{c1}(3872) \rightarrow \pi^+\pi^-\chi_{c1}]$ measurement at each c.m. energy is calculated by adding them in quadrature, as listed in the last column of Table I. Table III in Appendix B summarizes the systematic uncertainties for the $\sigma[e^+e^- \rightarrow \gamma\chi_{c1}(3872)]\mathcal{B}[\chi_{c1}(3872) \rightarrow \pi^+\pi^-\chi_{c1}]$ measurement.

In summary, with a data sample corresponding to an integrated luminosity of 10.9 fb $^{-1}$ collected with the BESIII detector at c.m. energies ranging from 4.16 to 4.34 GeV, the process $e^+e^- \rightarrow \gamma\chi_{c1}(3872)$ with $\chi_{c1}(3872) \rightarrow \pi^+\pi^-\chi_{c1}$ is studied, and no obvious signal is found. A 90% C.L. upper limit on the $\sigma[e^+e^- \rightarrow \gamma\chi_{c1}(3872)]\mathcal{B}[\chi_{c1}(3872) \rightarrow \pi^+\pi^-\chi_{c1}]$ is set at each c.m. energy. We also set a limit on the ratio of branching fractions of $\mathcal{R} = \frac{\mathcal{B}[\chi_{c1}(3872) \rightarrow \pi^+\pi^-\chi_{c1}]}{\mathcal{B}[\chi_{c1}(3872) \rightarrow \pi^+\pi^- J/\psi]} < 0.18$ at a 90% confidence level, which is consistent with the

measurement from the Belle Collaboration [39, 40]. Considering $\frac{\mathcal{B}[\chi_{c1}(3872) \rightarrow \pi^0 \chi_{c1}]}{\mathcal{B}[\chi_{c1}(3872) \rightarrow \pi^+ \pi^- J/\psi]} = 0.88^{+0.33}_{-0.27} \pm 0.10$ [9], the relative decay width $\frac{\Gamma[\chi_{c1}(3872) \rightarrow \chi_{c1} \pi^0]}{\Gamma[\chi_{c1}(3872) \rightarrow \chi_{c1} \pi^+ \pi^-]} > 5$ is determined, which is two orders of magnitude greater than that expected under a pure charmonium 2^3P_1 assumption for the $\chi_{c1}(3872)$ [16]. These measurements favor the non-conventional charmonium nature of the $\chi_{c1}(3872)$ state [17], and help to constrain the $c\bar{c}$ core component in the $\chi_{c1}(3872)$ wave function [41].

Acknowledgement

The BESIII Collaboration thanks the staff of BEPCII and the IHEP computing center for their strong support. This work is supported in part by National Key R&D Program of China under Contracts Nos. 2020YFA0406300, 2020YFA0406400; National Natural Science Foundation of China (NSFC) under Contracts Nos. 11975141, 11635010, 11735014, 11835012, 11935015, 11935016, 11935018, 11961141012, 12025502, 12035009, 12035013, 12061131003, 12192260, 12192261, 12192262, 12192263, 12192264, 12192265, 12221005, 12225509, 12235017; the Chinese Academy of Sciences (CAS) Large-Scale Scientific Facility Program; the CAS Center for Excellence in Particle Physics (CCEPP); Joint Large-Scale Scientific Facility Funds of the NSFC and CAS

under Contract No. U1832207; CAS Key Research Program of Frontier Sciences under Contracts Nos. QYZDJ-SSW-SLH003, QYZDJ-SSW-SLH040; 100 Talents Program of CAS; Project ZR2022JQ02 supported by Shandong Provincial Natural Science Foundation; Supported by the China Postdoctoral Science Foundation under Grant No. 2023M742100; The Institute of Nuclear and Particle Physics (INPAC) and Shanghai Key Laboratory for Particle Physics and Cosmology; European Union's Horizon 2020 research and innovation programme under Marie Skłodowska-Curie grant agreement under Contract No. 894790; German Research Foundation DFG under Contracts Nos. 455635585, Collaborative Research Center CRC 1044, FOR5327, GRK 2149; Istituto Nazionale di Fisica Nucleare, Italy; Ministry of Development of Turkey under Contract No. DPT2006K-120470; National Research Foundation of Korea under Contract No. NRF-2022R1A2C1092335; National Science and Technology fund of Mongolia; National Science Research and Innovation Fund (NSRF) via the Program Management Unit for Human Resources & Institutional Development, Research and Innovation of Thailand under Contract No. B16F640076; Polish National Science Centre under Contract No. 2019/35/O/ST2/02907; The Swedish Research Council; U. S. Department of Energy under Contract No. DE-FG02-05ER41374

-
- [1] S. K. Choi *et al.* [Belle Collaboration], Phys. Rev. Lett. **91**, 262001 (2003).
- [2] R. L. Workman *et al.* [Particle Data Group], PTEP **2022**, 083C01 (2022).
- [3] M. Ablikim *et al.* [BESIII Collaboration], Phys. Rev. Lett. **130**, 151904 (2023)
- [4] B. Aubert *et al.* [BaBar Collaboration], Phys. Rev. D **71**, 071103 (2005); R. Aaij *et al.* [LHCb Collaboration], JHEP **08**, 123 (2020).
- [5] M. Ablikim *et al.* [BESIII Collaboration], Phys. Rev. Lett. **112**, 092001 (2014).
- [6] B. Aubert *et al.* [BaBar Collaboration], Phys. Rev. D **77**, 011102 (2008); T. Aushev *et al.* [Belle Collaboration], Phys. Rev. D **81**, 031103 (2010).
- [7] M. Ablikim *et al.* [BESIII Collaboration], Phys. Rev. Lett. **124**, 242001 (2020).
- [8] B. Aubert *et al.* [BaBar Collaboration], Phys. Rev. D **74**, 071101 (2006); V. Bhardwaj *et al.* [Belle Collaboration], Phys. Rev. Lett. **107**, 091803 (2011); R. Aaij *et al.* [LHCb Collaboration], Nucl. Phys. B **886**, 665-680 (2014).
- [9] M. Ablikim *et al.* [BESIII Collaboration], Phys. Rev. Lett. **122**, 202001 (2019).
- [10] P. del Amo Sanchez *et al.* [BaBar Collaboration], Phys. Rev. D **82**, 011101 (2010).
- [11] M. Ablikim *et al.* [BESIII Collaboration],
- [12] L. Maiani, F. Piccinini, A. D. Polosa and V. Riquer, Phys. Rev. D **71**, 014028 (2005); A. Esposito, A. L. Guerrieri, F. Piccinini, A. Pilloni and A. D. Polosa, Int. J. Mod. Phys. A **30**, 1530002 (2015).
- [13] T. Barnes, S. Godfrey and E. S. Swanson, Phys. Rev. D **72**, 054026 (2005).
- [14] E. S. Swanson, Phys. Rept. **429**, 243 (2006).
- [15] F. K. Guo, C. Hanhart, U. G. Meißner, Q. Wang, Q. Zhao and B. S. Zou, Rev. Mod. Phys. **90**, 015004 (2018).
- [16] S. Dubynskiy and M. B. Voloshin, Phys. Rev. D **77**, 014013 (2008).
- [17] S. Fleming and T. Mehen, Phys. Rev. D **78**, 094019 (2008).
- [18] M. Ablikim *et al.* [BESIII Collaboration], Nucl. Instrum. Meth. A **614**, 345 (2010).
- [19] M. Ablikim *et al.* [BESIII Collaboration], Chin. Phys. C **40**, 063001 (2016); Chin. Phys. C **45**, 103001 (2021).
- [20] M. Ablikim *et al.* [BESIII Collaboration], Chin. Phys. C **46**, 113002 (2022)
- [21] C. H. Yu *et al.*, Proceedings of IPAC2016, Busan, Korea, 2016, doi:10.18429/JACoW-IPAC2016-TUYA01.
- [22] K. X. Huang, *et al.*, Nucl. Sci. Tech. **33**, 142 (2022).
- [23] X. Li *et al.*, Radiat. Detect. Technol. Methods **1**, 13 (2017); Y. X. Guo *et al.*, Radiat. Detect. Technol. Methods **1**, 15 (2017); P. Cao *et al.*, Nucl. Instrum. Meth. A **953**, 163053 (2020).
- [24] S. Agostinelli *et al.* (GEANT4 Collaboration), Nucl. Instrum. Meth. A **506**, 250 (2003).
- [25] D. J. Lange, Nucl. Instrum. Meth. A **462**, 152 (2001); R. G. Ping, Chin. Phys. C **32**, 599 (2008).
- [26] S. Jadach, B. F. L. Ward, and Z. Was, Comput. Phys. Commun. **130**, 260 (2000).
- [27] E. Richter-Was, Phys. Lett. B **303**, 163 (1993); P. Golonka, and Z. Was, Eur. Phys. J. C **45**, 97 (2006).
- [28] J. C. Chen, G. S. Huang, X. R. Qi, D. H. Zhang and Y. S. Zhu, Phys. Rev. D **62**, 034003 (2000); R. L. Yang, R. G. Ping and H. Chen, Chin. Phys. Lett. **31**, 061301 (2014).
- [29] X. Zhou, S. Du, G. Li and C. Shen, Comput. Phys. Commun. **258**, 107540 (2021).
- [30] M. Ablikim *et al.* [BESIII Collaboration], Phys. Rev. D **101**, 012008 (2020).

- [31] M. Ablikim *et al.* [BESIII Collaboration], Phys. Rev. Lett. **129**, 102003 (2022).
- [32] C. Rover, C. Messenger and R. Prix, doi:10.5170/CERN-2011-006.158.
- [33] Wolfgang A. Rolke, Angel M. Lopez, and Jan Conrad, Nucl. Instrum. Meth. A **551**, 493 (2005).
- [34] M. Ablikim *et al.* [BESIII Collaboration], Phys. Rev. D **81**, 052005 (2010).
- [35] W. L. Yuan, X. C. Ai, X. B. Ji, S. J. Chen, Y. Zhang, L. H. Wu, L. L. Wang and Y. Yuan, Chin. Phys. C **40**, 026201 (2016).
- [36] M. Ablikim *et al.* [BESIII Collaboration], Phys. Rev. Lett. **118**, 092001 (2017).
- [37] M. Ablikim *et al.* [BESIII Collaboration], Phys. Rev. D **87**, 012002 (2013).
- [38] W. Sun, T. Liu, M. Jing, L. Wang, B. Zhong and W. Song, Front. Phys. (Beijing) **16**, 64501 (2021).
- [39] V. Bhardwaj *et al.* [Belle Collaboration], Phys. Rev. D **93**, 052016 (2016).
- [40] S. K. Choi *et al.* [Belle Collaboration], Phys. Rev. D **84**, 052004 (2011).
- [41] M. Takizawa and S. Takeuchi, PTEP, **2013**, 093D01 (2013).

Appendix A: The distribution of $M^{\text{recoil}}(\gamma_{\text{rad}})$ at each c.m. energy

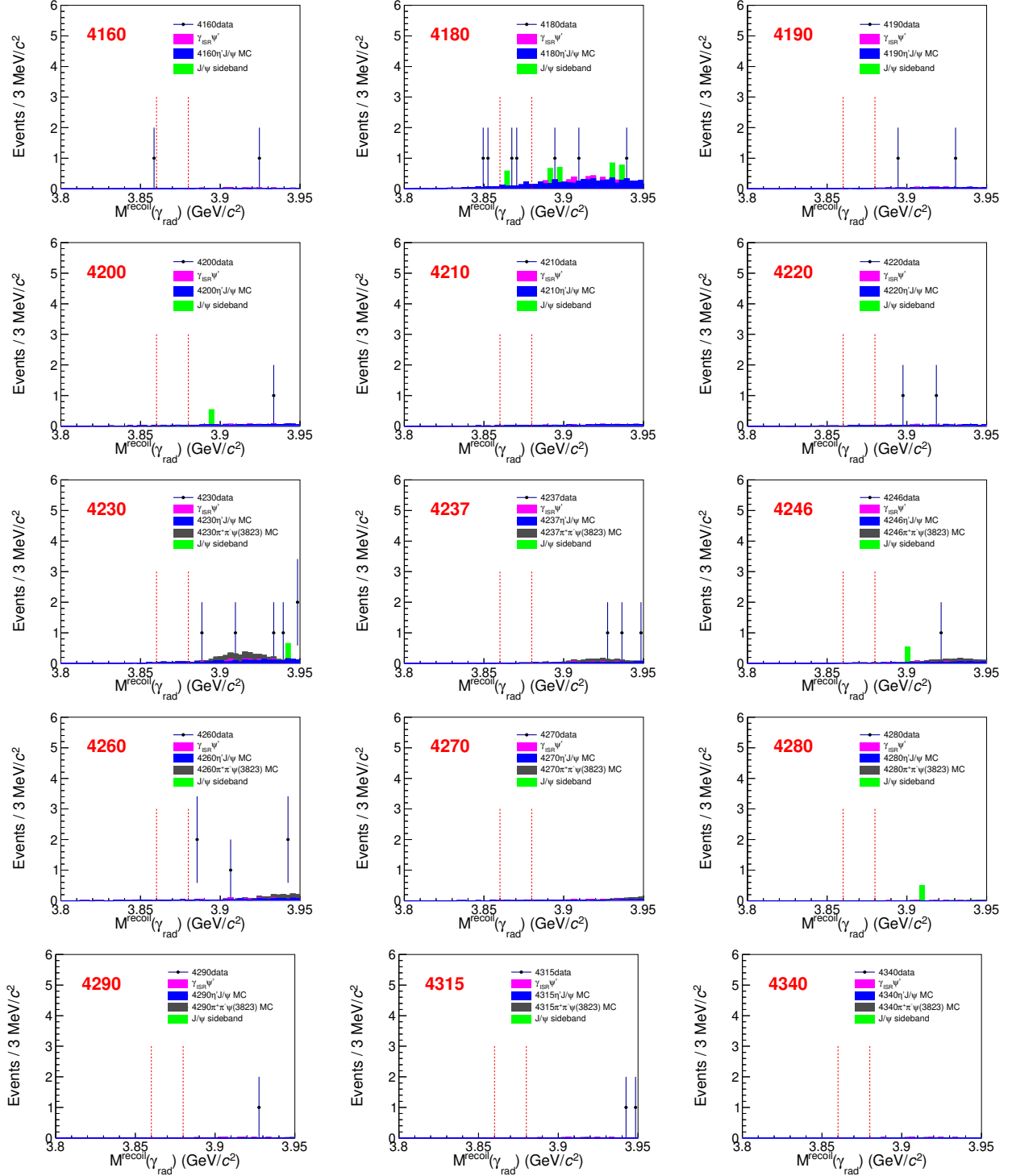


FIG. 3. The distribution of $M^{\text{recoil}}(\gamma_{\text{rad}})$ at each c.m. energy from 4.16 GeV to 4.34 GeV. For each c.m. energy, the 3-track events and 4-track events are combined together. Black dots with error bars are data, pink histogram is $\gamma_{\text{ISR}}\psi'$ MC, blue histogram is $\eta' J/\psi$ MC, black histogram is $\pi^+\pi^-\psi(3823)$ MC and green histogram is J/ψ sideband. The red dotted line represents the signal region of $\chi_{c1}(3872)$.

Appendix B: Systematic uncertainty for cross section measurement

TABLE III. Systematic uncertainties (in %) for the $\sigma[e^+e^- \rightarrow \gamma\chi_{c1}(3872)]\mathcal{B}[\chi_{c1}(3872) \rightarrow \pi^+\pi^-\chi_{c1}]$ measurement. The sources marked with "*" are shared systematic uncertainties for different data sets.

Data set	4160	4180	4190	4200	4210	4220	4230	4237	4246	4260	4270	4280	4290	4315	4340
Luminosity*	0.7	0.7	0.7	0.7	0.7	0.7	0.7	0.7	0.7	0.7	0.7	0.7	0.7	0.7	0.7
Photon efficiency*	2.0	2.0	2.0	2.0	2.0	2.0	2.0	2.0	2.0	2.0	2.0	2.0	2.0	2.0	2.0
Tracking efficiency*	2.0	2.0	2.0	2.0	2.0	2.0	2.0	2.0	2.0	2.0	2.0	2.0	2.0	2.0	2.0
PID*	0.5	0.5	0.5	0.5	0.5	0.5	0.5	0.5	0.5	0.5	0.5	0.5	0.5	0.5	0.5
$\mathcal{B}(\chi_{c1} \rightarrow \gamma J/\psi)^*$	3.0	3.0	3.0	3.0	3.0	3.0	3.0	3.0	3.0	3.0	3.0	3.0	3.0	3.0	3.0
$\mathcal{B}(J/\psi \rightarrow e^+e^-/\mu^+\mu^-)^*$	0.6	0.6	0.6	0.6	0.6	0.6	0.6	0.6	0.6	0.6	0.6	0.6	0.6	0.6	0.6
J/ψ mass window*	0.3	0.3	0.3	0.3	0.3	0.3	0.3	0.3	0.3	0.3	0.3	0.3	0.3	0.3	0.3
Kinematic fit	1.2	1.0	1.1	1.1	1.2	1.0	1.0	1.1	1.0	1.1	1.1	1.2	1.0	1.2	1.4
MC decay model*	2.8	2.8	2.8	2.8	2.8	2.8	2.8	2.8	2.8	2.8	2.8	2.8	2.8	2.8	2.8
Radiative correction	0.4	1.3	1.7	1.8	1.6	1.7	1.4	1.5	1.5	1.5	1.5	1.9	1.6	1.6	1.7
Total	5.3	5.4	5.5	5.5	5.5	5.5	5.4	5.5	5.4	5.4	5.5	5.6	5.5	5.5	5.6